

# Calculating the ‘Chain Splay’ of Amphiphilic Molecules: Towards Quantifying the Molecular Shapes

Chandrashekhar V. Kulkarni\*

*School of Physical Sciences and Computing, University of Central Lancashire, Preston, PR1 2HE, United Kingdom.*

\*Corresponding author E-mail [cvkulkarni@uclan.ac.uk](mailto:cvkulkarni@uclan.ac.uk), Tel: +44-1772-89-4339, Fax: +44-1772-89-4981.

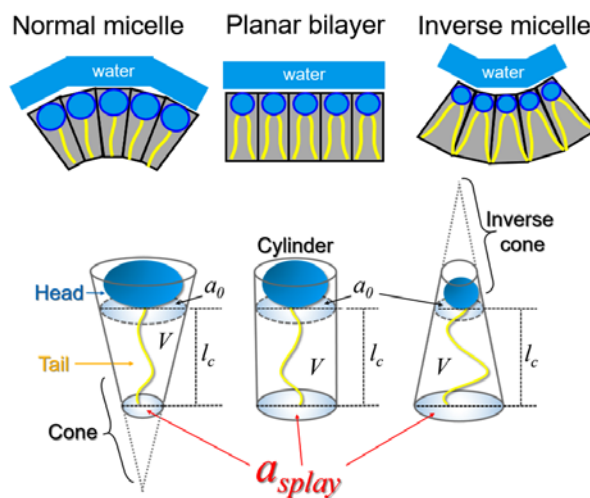
## Abstract

We report the first method to calculate a very important molecular level parameter of amphiphilic molecules– the ‘chain splay’. The calculations employed a *truncated cone* geometry, as it is the most probable configuration adopted by various amphiphiles. This approach utilized known parameters including lipid length, cross-sectional area at the head group and molecular volume. This new parameter, i.e. the area at the chain end, perceived to be more sensitive than Israelachvili’s famous shape factor or critical packing parameter (CPP). With relevant calculations, we demonstrate the fundamental roles of ‘chain splay’ to: a) reveal the critical contribution of molecular structure on average molecular shape and consequent self-assemblies, b) track the finest changes in molecular shapes within different bicontinuous cubic phases, c) obtain non-zero areas at the chain ends of amphiphiles that form *normal (type 1)* phases, d) back-calculate molecular volumes close to theoretical values, and e) find the link between molecular shapes and global curvatures of self-assemblies. This powerful feature advances our abilities towards quantitative estimation of spatial configurations adopted by amphiphilic molecules; moreover, it has a strong impact on predicting biomembrane structuring and nanoscale design of corresponding self-assemblies for a range of emerging applications.

## Keywords

Chain splay; biomembrane structures; average molecular shape; critical packing parameter; lipid self-assembly

## Graphical Abstract



## Introduction

### Molecular Shapes and Self-assembly of Amphiphilic Molecules

Amphiphilic molecules exhibit hydrophilic and hydrophobic parts, which allow them to self-assemble into an extensive range of structures when mixed with water (Seddon and Templer, 1995; Tiddy, 1980). Lipid molecules, constituting complex biomembrane architectures, foods and cosmetics, as well as, surfactants, consumed in daily (e.g. cleaning) applications are best examples of these (Chernik, 1999; de Kruijff, 1997; Kulkarni, 2016; Kulkarni, 2012; Leser et al., 2006; Rhein et al., 2006; Tiddy, 1980). Average molecular shapes adopted by amphiphilic molecules within the corresponding self-assemblies are qualitatively described by Israelachvili's famous shape factor or critical packing parameter, CPP ( $\gamma$ ) (Israelachvili, 1991; Israelachvili et al., 1976), which is expressed with *equation 1*. Optimum values of  $V$ - molecular volume,  $a_0$  - cross-sectional area at the hydrocarbon-water interface and  $l_c$  - chain length (Figure 1) form the basis of this equation.

$$\gamma = V/a_0l_c \quad (1)$$

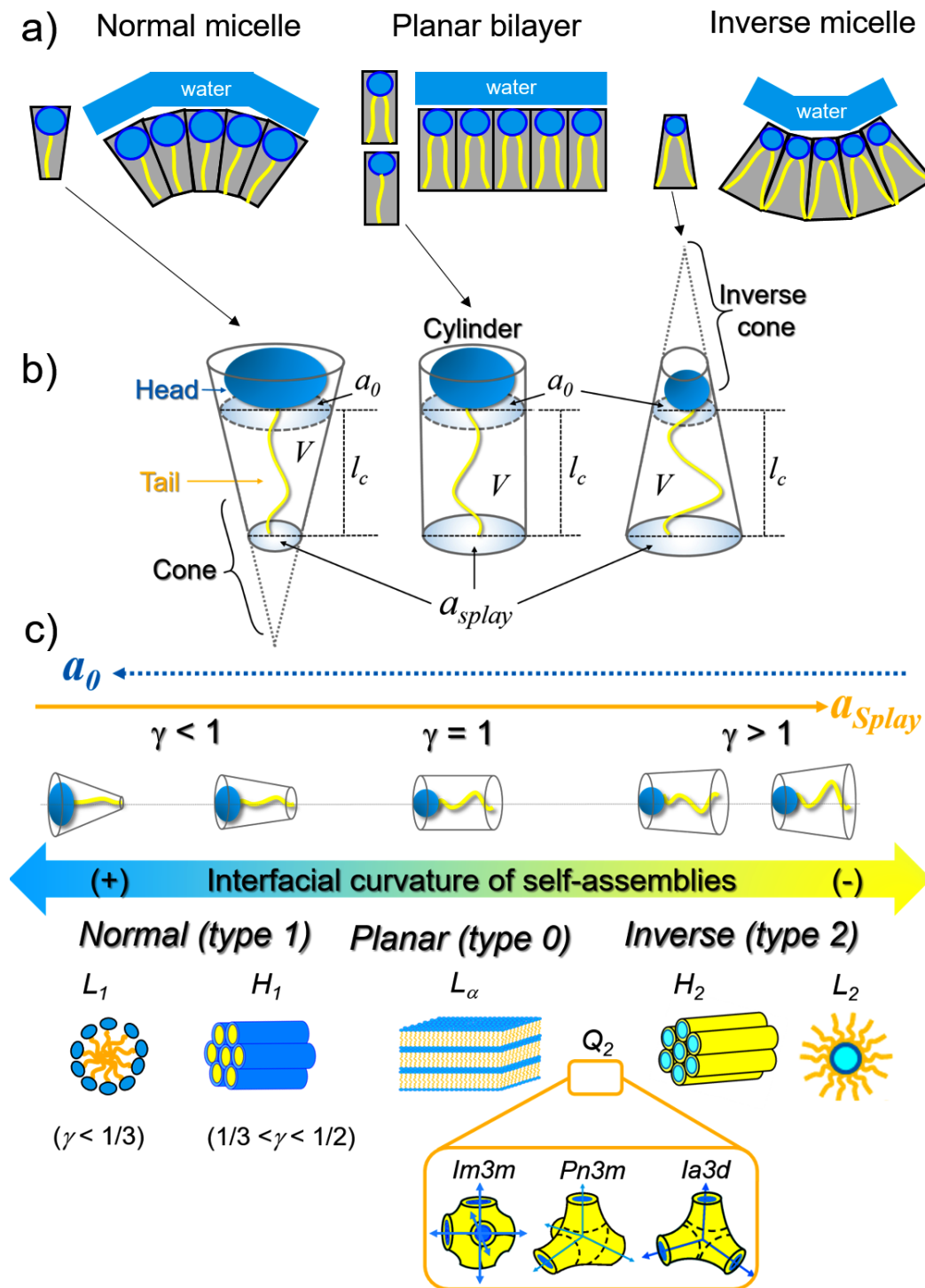


**Figure 1. Molecular shapes of amphiphilic molecules.** a) 2-D representation of typical micellar shapes formed by amphiphilic molecules. b) Surfactants commonly adopt conical shape while majority of lipids display inverse conical shapes; some lipids and surfactants also adapt cylindrical shapes, particularly when the cross-sectional area at the head group and tail are equal. The critical packing parameter (CPP), indicated usually by  $\gamma$ , is defined (equation 1) using optimum area per lipid at the interface ( $a_0$ ), optimum chain length ( $l_c$ ) and the optimum molecular volume ( $V$ ). The splay area ( $a_{splay}$ ) designates the area at the chain end. Solid grey lines depict truncated cone and cylindrical geometries. c) Normal (type 1) phases including spherical ( $L_1$ ) and cylindrical (e.g. hexagonal phase,  $H_1$ ) micelles are formed by conical molecules; planar phases (e.g. fluid lamellar,  $L_\alpha$ ) are formed by cylindrical molecules whereas

inverse conical molecules tend to form *inverse (type 2)* bicontinuous cubic phases ( $Q_2$ ) with typical space groups  $Im3m$ ,  $Pn3m$  and  $Ia3d$ , hexagonal ( $H_2$ ) and inverse micellar ( $L_2$ ) phases. An average interfacial curvature is considered positive (+) when the curvature is towards chain region while it is negative (-) when it is opposite, i.e. towards head group or aqueous region. The value of  $a_{splay}$  is greater than  $a_o$  for inverse phases, equal for planar phases and lesser for normal phases as indicated by solid and dotted arrows, respectively for increasing directions of  $a_{splay}$  and  $a_o$ . Schematic diagrams of self-assembled phases and molecular shapes are drawn for illustration purpose only (not on the scale).

The value of  $\gamma$  is below 1 for *normal (type 1)* phases and the molecule adopts a ‘cone’ shape whereas it is greater than 1 for *inverse (type 2)* phases and the molecule adopts an ‘inverted cone’ shape (Figure 1) (Israelachvili et al., 1976). Cylindrical molecules exhibit  $\gamma$  values of about 1 (Figure 1) forming *planar (type 0)* phases. Different  $\gamma$  values further rationalize the effective shapes adopted by amphiphilic self-assemblies; for instance,  $\gamma$  is  $< 1/3$  for spherical micelles ( $L_1$ ),  $1/3$  to  $1/2$  for cylindrical shapes (e.g. hexagonal phase,  $H_1$ ) and  $1/2$  to 1 for bilayer-based *type 1* phases (Figure 1) (Israelachvili, 1991; Israelachvili et al., 1976). However, this rationalization is not beneficial for differentiating inverse phases (where  $\gamma > 1$ ), although they display a remarkable range of polymorphism including cylindrical, spherical and bilayer-based architectures (Luzzati et al., 1968; Seddon, 1990; Seddon and Templer, 1995), respective examples of which would be hexagonal ( $H_2$ ), inverse micellar ( $L_2$ ), and bicontinuous cubic phases ( $Q_2$ ) of  $Im3m$ ,  $Pn3m$  and  $Ia3d$  types (Figure 1). (It is important to note that the discussion on ‘self-assembling’ and ‘molecular shapes’, throughout this report, is based on amphiphilic molecules that typically exhibit high aspect-ratios and consist (at least one) long hydrocarbon chain/s (generally longer than  $C_8$ ). The report does not focus other amphiphiles including bile salts (Madenci and Egelhaaf, 2010), peptides, membrane proteins and block-copolymers).

The geometric structure of the self-assembly (at global or meso scale) is strongly governed by the local shape of an amphiphile (at molecular level) (Figure 1). This relationship can be conveniently described by another expression for molecular shape parameter ( $\gamma$ ) using interfacial curvatures of the self-assembly as follows (equation 2) (Hyde et al., 1996; Hyde, 2001),

$$\gamma = 1 + |\langle H \rangle| l_c + |\langle K \rangle| l_c^2 / 3 \quad (2)$$

where,  $|\langle H \rangle|$  and  $|\langle K \rangle|$  represent average mean curvature modulus and average Gaussian curvature modulus, respectively. *Planar* surfaces, like lamellar phases (e.g.  $L_\alpha$ ) have zero mean ( $\langle H \rangle = 0$ ) and Gaussian ( $\langle K \rangle = 0$ ) curvatures, *normal* phases have positive mean ( $\langle H \rangle > 0$ ) curvature and *inverse* phases have negative mean curvature ( $\langle H \rangle < 0$ ) (Figure 1); ultimate

molecular shapes configured within these self-assemblies are cylindrical, conical and inverse conical, respectively, as depicted pictorially in [Figure 1](#) (Hyde, 2001). However, the molecular shape depiction, in the form of  $\gamma$ , is constrained to ‘qualitative’ rather than ‘quantitative’ estimation. In most cases, the  $\gamma$  is insensitive or fairly less sensitive to structural and environmental changes; in fact, it was reported to be more dependent on the chosen lipid length than the volume and the cross-sectional area of the molecule (Israelachvili et al., 1976). Some researchers have investigated other molecular scale parameters, including neutral surface area (Chung and Caffrey, 1994; Kozlov and Winterhalter, 1991; Templer, 1995; Winterhalter and Helfrich, 1992) and pivotal surface area (Marsh, 2011; Pisani et al., 2001; Tang et al., 2014) of selected amphiphilic molecules but these parameters are poor in realizing the molecular dimensions in the chain-end region (Chung and Caffrey, 1994; Kozlov and Winterhalter, 1991; Pisani et al., 2001; Templer, 1995; Winterhalter and Helfrich, 1992).

### **Suitability of ‘Truncated Cone Geometry’ for Amphiphilic Molecules**

For *normal* phases, the polar (hydrophilic) head group occupies the circular base of a cone while the (hydrophobic) chain/tail-end extends until the apex (vertex that is not on the base). On the other hand, molecules in *inverse* phases assume inverse conical shape where the chain-end region constitutes the base of a cone that becomes tapered towards the head group region ([Figure 1](#)). In fact, the actual molecular geometry adopted by *inverse* phases appears more like a ‘truncated cone’ or ‘frustum of a cone’ where the lipid chain region occupies larger area ( $a_{splay}$ ) of a truncated cone ([Figure 1](#)) (Israelachvili et al., 1980; Thurmond et al., 1993). This is attributed, theoretically, to the fact that the cross-sectional area at the head group ( $a_0$ ) does not reduce to zero (to reach an apex of the inverse cone). Although a few authors mentioned about the possible applicability of the *truncated cone* geometry (Carnie et al., 1979; Escribá, 2006; Israelachvili et al., 1980; Thurmond et al., 1993), it was never employed to calculate molecular shape parameters, in general. The practical knowledge of both,  $a_0$  and  $a_{splay}$  for amphiphilic self-assemblies, especially for inverse phases is indeed beneficial for more precise estimation of average molecular shapes assumed by self-assembled structures.

Here, we report a method to calculate  $a_{splay}$  (chain splay area) and  $r_{splay}$  (radius of chain splay area) with an understanding that the amphiphilic molecules adopt a *truncated cone* geometry. By evaluating the values of  $a_0$  and  $a_{splay}$  we effectively track the role of unsaturation on the effective molecular shapes of selected monoglycerides, which were qualitatively assessed previously by some research groups (Fong et al., 2012; Kulkarni et al., 2010). Finally, we

examine the suitability of *truncated cone* method for calculating molecular parameters for *normal* (type 1) phases, including spherical and cylindrical micelles (Figure 1). Development of a systematic model for perceiving the molecular chain splay, for the first time, is highly promising step towards the quantitative assessment of molecular shapes of amphiphilic molecules. It also opens up new avenues in our understanding of the individual roles of small complex molecules in biomembrane structuring as well as designing self-assemblies for biotechnological applications.

The volume ( $V$ ) of a *truncated cone* can be expressed using equation 3.

$$V = \frac{1}{3}\pi l_c(r_{splay}^2 + r_{splay}r_0 + r_0^2) \quad (3)$$

Absolute values of molecular volumes ( $V$ ) can be obtained from molecular models (Angelov et al., 1999) or calculated using standard formula (Supplementary Information-SI, equation S3) when the densities of the components under given conditions are known. The lipid chain length ( $l_c$ ) can be calculated from small angle X-ray scattering analysis (Clerc and Dubois-Violette, 1994; Rappolt, 2010), molecular models (Angelov et al., 1999) and/or using the known equations (listed in SI). Area per lipid at the interface ( $a_0$ ) can be calculated using molecular models (Angelov et al., 1999) or set of established equations (Kulkarni et al., 2011) (listed in SI). On the basis of known parameters  $V$ ,  $l_c$  and  $r_0$  (obtained from  $a_0 = \pi r_0^2$ ), the values of  $r_{splay}$  and  $a_{splay}$  (obtained from  $a_{splay} = \pi r_{splay}^2$ ) can be obtained by solving equation 3. Parameters, calculated in this manner, are presented in Table 1 for some of the representative examples of important lipids and surfactants (including cholesterol and selected phospholipids) that form *normal*, *inverse* and *planar* self-assemblies.

**Table 1. Chain splay of various lipids and surfactants.**

Amphiphilic molecule (Abbreviation)	Identity of self-assembly (space group)	Type of phase	A	B	C	D	E	F	G
			Volume $V^*$ $\text{\AA}^3$	Length $l_c^*$ $\text{\AA}$	Interfacial area $a_0^*$ $\text{\AA}^2$	Splay area $a_{splay}$ $\text{\AA}^2$	CPP $\gamma$	Recalculated Volume ( $V_{RC1}$ ) with $r_{splay} \neq 0$	Recalculated Volume ( $V_{RC2}$ ) with $r_{splay} = 0$
Cholesterol	$H_2$	Type 2	400.0	17.5	19.0	27.0	1.20	400.1	110.8
DOPE	$H_2$	Type 2	953.0	18.6	46.0	56.7	1.11	953.1	285.2
DPoIPC	Lamellar	Type 0	1184.8	16.6	71.4	71.4	1.00	1184.8	394.9
DOPC <sup>a</sup>	Lamellar	Type 0	1295.4	17.4	74.3	74.3	1.00	1295.4	431.8
DMPC	Lamellar	Type 0	1089.9	16.8	64.9	64.9	1.00	1089.8	363.3
Egg PC <sup>b</sup>	Vesicle/lamellar	Type 1 <sup>†</sup>	1063.0	19.0	71.7	41.6	0.78	1063.0	454.1
Egg PC <sup>b,c</sup>	Vesicle/lamellar	Type 1 <sup>†</sup>	1063.0	17.5	71.7	50.4	0.85	1063.8	418.3
Egg PC <sup>b</sup>	Vesicle/lamellar	Type 1 <sup>†</sup>	1063.0	16.0	71.7	61.3	0.93	1063.0	382.4
DPPC	Vesicle/lamellar	Type 1 <sup>†</sup>	871.0	17.6	60.0	39.7	0.82	871.1	352.0
OG	Cylindrical micelle	Type 1	245.0	9.3	37.0	17.0	0.71	245.0	114.7
OG	Spherical micelle	Type 1	245.0	9.3	55.0	6.0	0.48	245.1	170.5
LysoPC	Spherical micelle	Type 1	531.0	17.5	71.7	3.5	0.42	531.0	418.3

Molecular level parameters including chain splay area ( $a_{splay}$ ) and CPP ( $\gamma$ ) were calculated using known quantities\* obtained/calculated from corresponding references, for Cholesterol(Carnie et al., 1979), DOPE (dioleoylphosphatidylethanolamine)(Angelov et al., 1999), DPoIPC (dipalmitoleoylphosphatidylcholine)(Costigan

et al., 2000), DOPC/EggPC (dioleoylphosphatidylcholine)<sup>a</sup>(Costigan et al., 2000)<sup>b</sup>(Israelachvili et al., 1976)<sup>c</sup>(Carnie et al., 1979), DMPC (dimyristoylphosphatidylcholine)(Costigan et al., 2000), DPPC (dipalmitoylphosphatidylcholine)(Angelov et al., 1999), OG(Angelov et al., 1999) and LysoPC (lysophosphatidylcholine)(Carnie et al., 1979). The molecular volumes,  $V_{RC1}$  (column F) and  $V_{RC2}$  (column G) were recalculated (using [equation 3](#)) by assuming the molecules adopting *truncated cone* geometry and perfectly conical shapes respectively, i.e. when  $a_{splay} \neq 0$  and  $a_{splay} = 0$ . The *type I* phases: vesicles are usually formed by diverse molecules, i.e. by *type 1*, *2* and *0* structure forming amphiphiles; however, intuitively the practicality is either or a combination of the following – an average structure adopted by molecules is either *type 1* or the number of lipids in outer leaflet is more than the number of lipids in inner leaflet. Hence, the  $a_{splay}$  values for the vesicles were found to be smaller than  $a_{splay}$ . Chemical structures of the listed molecules are provided in SI.

The values of  $a_{splay}$ , obtained using [equation 3](#), were foreseeably greater than  $a_0$  for *type 2* phases and almost equal for *type 0* phases ([Table 1](#)). Cholesterol and DOPE (dioleoylphosphatidylethanolamine) form inverse hexagonal phase ( $H_2$ ) by adopting inverse conical molecular shapes, as evident from  $a_{splay} > a_0$  and  $\gamma > 1$  ([Table 1](#)). Other double-chained phospholipids, DPoIPC (dipalmitoleoylphosphatidylcholine), DOPC (dioleoylphosphatidylcholine) and DMPC (dimyristoylphosphatidylcholine) form lamellar (*type 0*) phases constituting planar bilayers. This is elucidated by practically equal values of  $a_{splay}$  and  $a_0$ , and by adoption of the cylindrical molecular shape with  $\gamma = 1$  ([Table 1](#)). Vesicles are bilayer-based assemblies, which when grow to extremely large sizes (e.g. giant unilamellar vesicles with typical size  $>1 \mu\text{m}$ ) adopt locally planar bilayer structures ( $\gamma$  values appearing towards unity, see [Table 1](#)). Average molecular shape is thus somewhere between planar and *truncated cone* shapes with  $a_{splay} \leq a_0$  on an average scale ([Table 1](#)) for DOPC and DPPC (dipalmitoylphosphatidylcholine) vesicles; while opposite might be also possible ( $a_{splay} \geq a_0$ ). Israelachvili et al. tracked molecular level changes in the growing vesicle formed by a double chain lipid, egg PC (Israelachvili et al., 1976) (DOPC) in water. At constant interfacial molecular area ( $71.7 \text{ \AA}^2$ ) and molecular volume ( $1063 \text{ \AA}^3$ ), the swelling vesicle absorbs increasing amount of water while decreasing an interfacial bilayer curvature. This is compensated by straightening of molecules via adopting more cylindrical geometries. The packing parameter,  $\gamma$  rises from 0.78 to 0.93, potentially reaching unity, as symbolized by locally planar phases.

Octylglucoside (OG), a surfactant, is known to form *normal* phases (Angelov et al., 1999) with  $\gamma$  values below 1. In presence of polar solvents, OG molecules acquire conical shapes because of their large polar head groups and rather short chains ( $C_8$ ). Interestingly enough, it was also possible to apply *truncated cone* geometry and obtain non-zero values of  $a_{splay}$  for amphiphiles displaying *type 1* phases, including OG and LysoPC (lysophosphatidylcholine) ([Table 1](#)). This

speculation perfectly aligns with the fact that the hydrocarbon chain end is usually occupied by a  $-CH_3$  group, and cannot be null. The volume of  $-CH_3$  group (Angelov et al., 1999) approximates to  $53.5 \text{ \AA}^3$ , meaning the cross-sectional area equals to about  $17.2 \text{ \AA}^2$ . The value of  $a_{splay}$  obtained from our calculations for cylindrical micelle (formed by OG) was practically same as this area ( $17.0 \text{ \AA}^2$ ; see Table 1). The  $a_{splay}$  for spherical micelles formed by OG and LysoPC were smaller than this value ( $6.0 \text{ \AA}^2$  and  $3.5 \text{ \AA}^2$ , respectively). More interestingly, by implementing *truncated cone* geometry to all of the aforementioned amphiphiles (and using  $l_c$ ,  $r_0$  and  $r_{splay}$ ), we were able to back-calculate  $V$  fairly accurately (see  $V_{RC1}$  in column F of Table 1), which was, however, found to be significantly deviated ( $V_{RC2}$  in column G of Table 1) from the absolute values (as in Column A of Table 1) when perfectly conical shape was implemented (i.e. by substituting  $a_{splay} = 0$  in equation 3). If, hypothetically, all self-assemblies were presumed to adopt perfectly conical shapes, where  $a_{splay} = 0$  (either *normal*, *planar* or *inverse* case) the recalculated volumes ( $V_{RC2}$ ) acquire erroneously low values (as low as  $\sim 28\%$  of the real volumes ( $V$ )) (Table 1). This further validates the appropriateness of *truncated cone* geometry for estimating shapes of various amphiphilic molecules over conventional conical or inverse conical shapes irrespective of their self-assembly type.

### **Retrospective Contribution of Molecular Chain Splay in Bicontinuous Cubic Phases (Monoelaidin-Water System)**

Monoelaidin (ME), a synthetic monoglyceride, contains *trans* double bond in the  $C_{18}$  alkyl chain attached to a glycerol backbone. The molecule adopts *truncated cone* shape and forms inverse self-assemblies (Kulkarni, 2011; Kulkarni et al., 2010). In presence of water, ME displays all three commonly found inverse bicontinuous cubic phases (Kulkarni, 2011; Kulkarni et al., 2010),  $Im3m$ ,  $Pn3m$  and  $Ia3d$ , based correspondingly on primitive (P), diamond (D) and Gyroid (G) type minimal surfaces (Andersson et al., 1988; Seddon and Templer, 1993; Seddon and Templer, 1995). Minimal surfaces are commonly distinguished by zero mean ( $H$ ) curvature and negative Gaussian ( $K$ ) curvature at every single point on it (Larsson, 1986). Bicontinuous cubic phases are formed by draping a continuous lipid bilayer around minimal surfaces, separating two different but continuous aqueous channels (Larsson, 1986). It is generally understood that the actual geometry attained by bilayers in cubic phases is an optimum blend of two models, namely, parallel interface model (PIM) which eliminates discrepancies in the lipid chain length and constant mean curvature (CMC) model which eliminates the discrepancies in the mean curvature (Chen and Jin, 2017). In the current work,

we prefer to use average values of molecular shapes, and consequently derived global curvatures for relevant self-assemblies.

In case of ME, the magnitude of average mean curvature ( $|\langle H \rangle|$ ) was found to increase from *Im3m* ( $0.01104 \text{ \AA}^{-1}$ ) to *Pn3m* ( $0.01506 \text{ \AA}^{-1}$ ) to *Ia3d* ( $0.02369 \text{ \AA}^{-1}$ ) phase, as commonly seen for a range of lipids (Andersson et al., 1988; Seddon and Templer, 1993; Seddon and Templer, 1995). Similarly, the Gaussian ( $|\langle K \rangle|$ ) curvature modulus increases from *Im3m* to *Pn3m* to *Ia3d* phase (Table 2). Apparent negative values of both curvatures indicate that the curvature is towards head group regions (Figure 1). Naturally, the *Ia3d* phase is expected to be formed of molecules whose CPP ( $\gamma$ ) has larger value compared to *Pn3m* having larger values with respect to *Im3m* phase. It means chain regions of molecules in *Ia3d* phase have larger average areas ( $a_{splay}$ ) compared to the cross-sectional areas at interfaces ( $a_0$ ) to accommodate higher global curvatures compared to other two phases. In other words, the chain splay ( $a_{splay}$ ) increases from *Im3m* ( $a_{splay}=38.33 \text{ \AA}^2$ ) to *Pn3m* ( $a_{splay}=39.02 \text{ \AA}^2$ ) to *Ia3d* ( $a_{splay}=40.15 \text{ \AA}^2$ ) phase (Table 2).

Among three cubic phases, *Im3m* has more (six) and larger water channels, and therefore it is anticipated to hold more water than *Pn3m* phase. Similar is also true when *Pn3m* (four channels) and *Ia3d* (three channels) phases are compared. Accordingly, the *Im3m* phase accommodates more water than *Pn3m* phase which can hold more water than *Ia3d* phase; thus apparent area ( $a_0$ ) in the hydrophilic head group region is higher for *Im3m* ( $a_0=31.16 \text{ \AA}^2$ ) than *Pn3m* ( $a_0=29.54 \text{ \AA}^2$ ) than *Ia3d* ( $a_0=26.24 \text{ \AA}^2$ ) phase (Table 2). This additional support, provided by greater  $a_0$  values while simultaneously securing lower  $a_{splay}$  values strongly benefit the molecules to compensate for lower curvatures of *Im3m* phase compared to *Pn3m* compared to *Ia3d* phase (Figure 1).

**Table 2. Comparison of chain splay in bicontinuous cubic phases of the same lipid.** Monoelaidin (ME) forms three bicontinuous cubic phases where *Im3m* is the least curved, *Pn3m* is the intermediate and *Ia3d* is the most curved phase (see magnitudes of  $\langle H \rangle$  and  $\langle K \rangle$ ). Apparent chain splay  $a_{splay}$  increases towards the most curved phase (*Ia3d*) while  $a_0$  increases towards least curved phase (*Im3m*).

Amphiphilic molecule (Abbreviation)	Identity of self-assembly (space group)	Volume $V^*$ $\text{\AA}^3$	Length $l_c^*$ $\text{\AA}$	Interfacial area $a_0^*$ $\text{\AA}^2$	Splay area $a_{splay}$ $\text{\AA}^2$	CPP $\gamma$	Average Mean Curvature ( $\langle H \rangle$ ) $\text{\AA}^{-1}$	Average Gaussian Curvature ( $\langle K \rangle$ ) $\text{\AA}^{-1}$
ME	<i>Im3m</i>	533.0	15.4	31.16	38.33	1.11	-0.01104	-0.00061
ME	<i>Pn3m</i>	533.0	15.6	29.54	39.02	1.16	-0.01506	-0.00078
ME	<i>Ia3d</i>	533.0	16.2	26.24	40.15	1.26	-0.02369	-0.00106

The small angle X-ray scattering (SAXS) data used for this analysis was adopted from reference(Kulkarni, 2011), generated under the following conditions: *Im3m* phase 45.5% water at 48 °C, *Pn3m* phase 36.3% water at 60 °C

and *Ia3d* phase 24.7% water at 60 °C (closely comparable data were picked ensuring the existence of pure phases under limited water conditions i.e. avoiding coexistence of phases and excess water boundaries).

The ratio (dimensionless) between splay area and interfacial area, i.e.  $a_{splay}/a_0$  is greater (1.23 for *Im3m*, 1.32 for *Pn3m* and 1.53 for *Ia3d* phase) than the conventional factor CPP ( $\gamma$ ), which is commonly used for describing molecular shapes of amphiphiles (Table 2). Moreover, the difference between these areas vary even more significantly, as much as almost double ( $a_{splay}-a_0=13.91 \text{ \AA}^2$ ) for *Ia3d* phase when compared to that of *Im3m* phase ( $a_{splay}-a_0=7.18 \text{ \AA}^2$ ) (Table 2). These results highlight an important fact that the chain splay is *more sensitive* than Israelachvili's CPP (Israelachvili, 1991; Israelachvili et al., 1976) in portraying molecular shapes that govern average curvatures of inverse cubic phases and, finally, in understanding the process of self-assembling of amphiphilic molecules.

### Effect of Unsaturation Characteristics on Chain Splay of Lipid Molecules

As mentioned earlier, ME forms three inverse bicontinuous cubic phases in presence of pure water (Kulkarni et al., 2010). Monoolein (MO) shares the same chemical formula as ME, but differs in the spacial orientation of the double bond (see chemical structures in SI). The *cis* arrangement in MO develops a kink in the molecule, which consequently increases the effective chain splay ( $a_{splay}=46.64 \text{ \AA}^2$ ). Due to *trans* conformation, ME exhibits rather straighter ( $a_{splay}/a_0=1.33$  for ME and 1.35 for MO) and longer ( $l_c=18.5 \text{ \AA}$  for ME;  $l_c=15.5 \text{ \AA}$  for MO) molecular shape than MO (Figure 2). Therefore, the least curved *Im3m* cubic phase, observed for ME-water system (Kulkarni, 2011) is not seen in MO-water phase diagram (Briggs et al., 1996). Moreover, the extended region occupied by planar lamellar phase/s and absence of more curved (than bicontinuous cubic phases) hexagonal phase in ME elucidate its straighter shape compared to MO (Briggs et al., 1996; Kulkarni, 2011). The *cis* double bond position in monovaccenein (MV) is altered from 9<sup>th</sup> (in MO) to 11<sup>th</sup> position, whose chain splay mediates ( $a_{splay}=43.45 \text{ \AA}^2$ ) the chain splay of ME and MO. The double bond, positioned at 9<sup>th</sup> place in MO, leaves longer chain (8-C chain) behind, which is likely to have higher degree of bending than the shorter one (6-C chain) in MV (Naudi et al., 2013). This could well be attributed to the elevated chain splay in MO with respect to MV. In case of monolinolein (ML), two *cis* unsaturations at 9<sup>th</sup> and 11<sup>th</sup> positions are responsible for two kinks causing substantial increase in the effective chain splay ( $a_{splay}=60.57 \text{ \AA}^2$ ); almost double  $a_{splay}$  than that of ME (Figure 2 and Table 3).

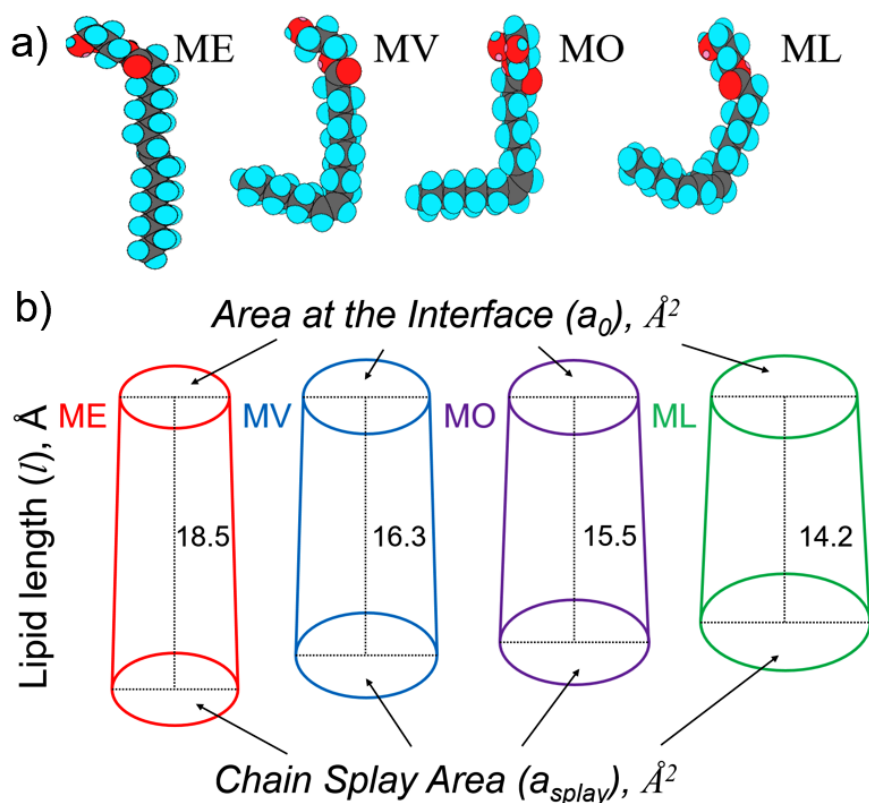


**Figure 2. Chain splay of single chain C<sub>18</sub> lipids differing in unsaturation characteristics.** a) ME contains *trans* isomerism at the double bond (at 9<sup>th</sup> position) while MO exhibits *cis* isomerism; MV consists *cis* double bond at 11<sup>th</sup> position whereas ML has two double bonds at C<sub>9</sub> and C<sub>11</sub> (Kulkarni et al., 2010). Not only  $a_{splay}$  increases from L to R but  $a_0$  also increases. However, the lipid lengths are decreased significantly (for absolute numbers see Table 3). b) In order to get a feel for alterations in molecular shapes, affected by unsaturation characteristics, the effective molecular shapes of lipids in a) are drawn on scale (with relative arbitrary units for calculated molecular parameters in Table 3).

The presence or absence of unsaturation/s in lipid molecules have strong impact on effective molecular packing, and also have considerable influence on the fluidity of biomembranes (Naudi et al., 2013; van Meer et al., 2008). Aforementioned chain splay variance caused due to unsaturation characteristics clearly supports this conception. The qualitative role of chain splay in stabilizing certain phases over others, and changes in aqueous channel dimensions were previously discussed by us (Kulkarni et al., 2010), and later by Fong et al. (Fong et al., 2012). In this report, we have quantified chain splay, in terms of absolute numbers, to better represent its role in the self-assembling of these unsaturated monoglycerides.

**Table 3. Quantifying the chain splay of homologous series of unsaturated lipids.**

Amphiphilic molecule	Identity of self-assembly (Abbreviation) (space group)	Volume $V^*$ ( $\text{\AA}^3$ )	Length $l_c^*$ ( $\text{\AA}$ )	Interfacial area $a_0^*$ ( $\text{\AA}^2$ )	Splay area $a_{splay}$ ( $\text{\AA}^2$ )	CPP $\gamma$	Average Mean Curvature $\langle\langle H \rangle\rangle$ ( $\text{\AA}^{-1}$ )	Average Gaussian Curvature $\langle\langle K \rangle\rangle$ ( $\text{\AA}^{-1}$ )
ME	$Pn3m$	533.4	18.5	24.80	32.96	1.16	-0.01318	-0.00057
MV	$Pn3m$	628.5	16.3	33.76	43.45	1.14	-0.01294	-0.00065
MO	$Pn3m$	628.5	15.5	34.65	46.64	1.17	-0.01647	-0.00085
ML	$Pn3m$	741.3	14.2	44.40	60.57	1.18	-0.01884	-0.00105

All values were calculated at 45 °C using the data from reference(Kulkarni et al., 2010). Chemical structures of the listed molecules are provided in SI.

It is essential to iterate that, the absolute values of CPP ( $\gamma$ ) do not show any trend as one moves from ME to ML (Table 3), revealing its inability to express unsaturation effects on molecular shapes. The area ratios ( $a_{splay}/a_0$ ) also do not display any particular preference. However, there was a clear growth in  $a_{splay}$ , as well as in  $a_0$  (from ME to ML). Opposite trend, i.e. the decay in lattice parameters ( $a=107 \text{ \AA}$  for ME,  $100 \text{ \AA}$  for MV,  $88 \text{ \AA}$  for MO and  $79 \text{ \AA}$  for ML; all at 45 °C) and reduction in lipid length ( $l_c$ ) (Table 3) was noticed from ME to ML. The overall molecular shapes of ME, MV, MO and ML influence the self-assembling at the global scale, as shown by elevation in average Gaussian curvatures ( $\langle\langle K \rangle\rangle$ ) (Table 3). These analyses demonstrate the significance of molecular level features ( $l_c$ ,  $a_0$  and  $a_{splay}$ ) in depicting a clear picture of molecular shapes adopted by amphiphilic molecules.

## Conclusions and Perspectives

We developed a new method for systematic calculation of the chain splay (area at the chain end,  $a_{splay}$ ) by employing a *truncated cone* geometry to describe molecular shapes of a range of amphiphilic molecules. Investigated molecules were selected carefully to cover a variety of self-assemblies including *normal*, *planar* and *inverse* phases. Several parameters, including  $V$ ,  $l_c$ ,  $a_0$ ,  $a_{splay}$ ,  $\gamma$ ,  $\langle\langle H \rangle\rangle$  and  $\langle\langle K \rangle\rangle$  were calculated using a set of established equations (some of which are listed in SI).

It can be decisively stated that the most probable shape assumed by a majority of amphiphilic molecules, including the ones that form *normal* phases, is a *truncated cone* geometry. Resultant non-zero values of  $a_{splay}$  for *normal* phases and accurate volumes ( $V$ ) recalculated by incorporating  $a_{splay}$  in *equation 3* explicitly prove this statement (Table 1). As mentioned earlier,  $\gamma$  only qualitatively interprets the molecular shapes, but by estimating the molecular chain splay, we have advanced at least one-step forward in quantifying the molecular shapes

of amphiphilic molecules. At times, when  $\gamma$  values do not render particular trends, for instance, for molecules with variable unsaturation properties (as reported in Figure 2, Table 3),  $a_{splay}$  demonstrates to be powerful and highly conclusive factor (a clear increase in  $a_{splay}$  was observed from ME to ML). It also corroborates well with the global curvature values (e.g.  $\langle K \rangle$  in Table 2 and Table 3) of cubic phases.

The values of  $a_{splay}$  and  $a_0$ , together, are capable of distinguishing finest changes in the shape of the same molecule, for example, of ME (Table 2). The molecular shape described by  $\gamma$  shows small variation (~13 % change in  $Ia3d$  with respect to  $Im3m$  phase), but the difference between  $a_{splay}$  and  $a_0$  outlines as high as 94 % change between these phases. With this, it is possible to get a better sketch of molecular shapes embraced by different bicontinuous cubic phases formed by the same molecule. The percentage change in  $a_{splay}-a_0$  varies monotonically (when compared with  $a_{splay}-a_0$  of ME) from MV (19 %) to MO (47 %) to ML (98 %) in the direction of increasing chain splay. These numbers demonstrate the sensitiveness of chain splay over the conventional shape parameter ( $\gamma$ ) and contribute towards deeper understanding of the effect of unsaturation. Our investigations quantitatively confirm previous observations by other researchers (Fong et al., 2012; Kulkarni et al., 2010), that not only the number but also the location of unsaturation in the hydrocarbon chain and the local conformation at the double bond are imperative in configuring lipid molecular shapes, their packing and stabilization of the consequent self-assemblies. This information is highly promising and relevant for understanding structural properties (e.g. packing, rigidity) and hence functioning of complex biomembranes, which are essentially composed of very distinct molecules. With the quantitative estimation of an important parameter, chain splay ( $a_{splay}$ ), the issue of packing frustration might be resolved in a better manner as it is dealt, specifically, with the chain region of curved lipid phases.

### **Conflicts of Interests**

There are no conflicts of interest to declare.

### **Acknowledgements**

We would like to thank Prof Michael Rappolt from University of Leeds (UK) for fruitful discussions, Dr Yogita Patil-Sen for initial support regarding preliminary calculations and Dr Vinod Kumar Vishwapathi for chemical structure drawings.

## References

- Andersson, S., Hyde, S.T., Larsson, K., Lidin, S., 1988. Minimal-Surfaces and Structures - from Inorganic and Metal Crystals to Cell-Membranes and Bio-Polymers. *Chemical Reviews* 88, 221-242.
- Angelov, B., Ollivon, M., Angelova, A., 1999. X-ray Diffraction Study of the Effect of the Detergent Octyl Glucoside on the Structure of Lamellar and Nonlamellar Lipid/Water Phases of Use for Membrane Protein Reconstitution. *Langmuir* 15, 8225-8234.
- Briggs, J., Chung, H., Caffrey, M., 1996. The temperature-composition phase diagram and mesophase structure characterization of the monoolein/water system. *J. Phys. II France* 6, 723-751.
- Carnie, S., Israelachvili, J.N., Pailthorpe, B.A., 1979. Lipid packing and transbilayer asymmetries of mixed lipid vesicles. *Biochim Biophys Acta* 554, 340-357.
- Chen, H., Jin, C., 2017. Competition brings out the best: modelling the frustration between curvature energy and chain stretching energy of lyotropic liquid crystals in bicontinuous cubic phases. *Interface Focus* 7, 20160114.
- Chernik, G.G., 1999. Phase studies of surfactant-water systems. *Current Opinion in Colloid & Interface Science* 4, 381-390.
- Chung, H., Caffrey, M., 1994. The neutral area surface of the cubic mesophase: location and properties. *Biophys. J.* 66, 377-381.
- Clerc, M., Dubois-Violette, E., 1994. X-ray scattering by bicontinuous cubic phases. *J. Phys. II France* 4, 275-286.
- Costigan, S.C., Booth, P.J., Templer, R.H., 2000. Estimations of lipid bilayer geometry in fluid lamellar phases. *Biochimica et Biophysica Acta-Biomembranes* 1468, 41-54.
- de Kruijff, B., 1997. Lipid polymorphism and biomembrane function. *Current Opinion in Chemical Biology* 1, 564-569.
- Escribá, P.V., 2006. Membrane-lipid therapy: a new approach in molecular medicine. *Trends in Molecular Medicine* 12, 34-43.
- Fong, C., Le, T., Drummond, C.J., 2012. Lyotropic liquid crystal engineering-ordered nanostructured small molecule amphiphile self-assembly materials by design. *Chemical Society reviews* 41, 1297-1322.
- Hyde, S., Blum, Z., Landh, T., Lidin, S., Ninham, B.W., Andersson, S., Larsson, K., 1996. *The Language of Shape: The Role of Curvature in Condensed Matter: Physics, Chemistry and Biology*. Elsevier Science.
- Hyde, S.T., 2001. Identification of lyotropic liquid crystalline mesophases, In: Holmberg, K. (Ed.), *Handbook of Applied Surface and Colloid Chemistry*. John Wiley & Sons, Ltd., pp. 299-332.
- Israelachvili, J., 1991. *Intermolecular and Surface Forces*. Academic Press, London.
- Israelachvili, J.N., Marčelja, S., Horn, R.G., 1980. Physical principles of membrane organization. *Quarterly reviews of biophysics* 13, 121-200.
- Israelachvili, J.N., Mitchell, D.J., Ninham, B.W., 1976. Theory of self-assembly of hydrocarbon amphiphiles into micelles and bilayers. *Journal of the Chemical Society, Faraday Transactions 2: Molecular and Chemical Physics* 72, 1525-1568.
- Kozlov, M.M., Winterhalter, M., 1991. Elastic moduli for strongly curved monolayers. Position of the neutral surface. *J. Phys. II France* 1, 1077-1084.
- Kulkarni, C., 2016. Lipid Self-Assemblies and Nanostructured Emulsions for Cosmetic Formulations. *Cosmetics* 3, 37.
- Kulkarni, C.V., 2011. Nanostructural studies on monoelaidin-water systems at low temperatures. *Langmuir* 27, 11790-11800.

- Kulkarni, C.V., 2012. Lipid crystallization: from self-assembly to hierarchical and biological ordering. *Nanoscale* 4, 5779-5791.
- Kulkarni, C.V., Tang, T.Y., Seddon, A.M., Seddon, J.M., Ces, O., Templer, R.H., 2010. Engineering Bicontinuous Cubic Structures at the Nanoscale– the Role of Chain Splay. *Soft Matter* 6, 3191-3194.
- Kulkarni, C.V., Wachter, W., Iglesias, G.R., Engelskirchen, S., Ahualli, S., 2011. Monoolein: A Magic Lipid? *Phys Chem Chem Phys* 13, 3004-3021.
- Larsson, K., 1986. Periodic minimal surface structures of cubic phases formed by lipids and surfactants. *Journal of Colloid and Interface Science* 113, 299-300.
- Leser, M.E., Sagalowicz, L., Michel, M., Watzke, H.J., 2006. Self-assembly of polar food lipids. *Advances in Colloid and Interface Science* 123-126, 125-136.
- Luzzati, V., Tardieu, A., Gulik-Krzywicki, T., 1968. Polymorphism of Lipids. *Nature* 217, 1028-1030.
- Madenci, D., Egelhaaf, S.U., 2010. Self-assembly in aqueous bile salt solutions. *Current Opinion in Colloid & Interface Science* 15, 109-115.
- Marsh, D., 2011. Pivotal surfaces in inverse hexagonal and cubic phases of phospholipids and glycolipids. *Chemistry and Physics of Lipids* 164, 177-183.
- Naudi, A., Jove, M., Ayala, V., Portero-Otin, M., Barja, G., Pamplona, R., 2013. Membrane lipid unsaturation as physiological adaptation to animal longevity. *Frontiers in physiology* 4, 372.
- Pisani, M., Bernstorff, S., Ferrero, C., Mariani, P., 2001. Pressure Induced Cubic-to-Cubic Phase Transition in Monoolein Hydrated System. *The Journal of Physical Chemistry B* 105, 3109-3119.
- Rappolt, M., 2010. Bilayer thickness estimations with “poor” diffraction data. *J Appl Phys* 107, 084701.
- Rhein, L.D., Schlossman, M., O'Lenick, A., Somasundaran, P., 2006. *Surfactants in Personal Care Products and Decorative Cosmetics*, Third Edition. CRC Press.
- Seddon, J.M., 1990. Structure of the inverted hexagonal (HII) phase, and non-lamellar phase transitions of lipids. *Biochimica et Biophysica Acta (BBA) - Reviews on Biomembranes* 1031, 1-69.
- Seddon, J.M., Templer, R.H., 1993. Cubic Phases of Self-assembled Amphiphilic Aggregates. *Philosophical transactions. Mathematical, physical, and engineering sciences* 344, 377-401.
- Seddon, J.M., Templer, R.H., 1995. Polymorphism of lipid-water systems, In: Lipowsky, R., Sackmann, E. (Eds.), *Handbook of Biological Physics*. Elsevier Science B.V. Amsterdam, pp. 97-160.
- Tang, T.Y.D., Seddon, A.M., Jeworrek, C., Winter, R., Ces, O., Seddon, J.M., Templer, R.H., 2014. The effects of pressure and temperature on the energetics and pivotal surface in a monoacylglycerol/water gyroid inverse bicontinuous cubic phase. *Soft Matter* 10, 3009-3015.
- Templer, R.H., 1995. On the Area Neutral Surface of Inverse Bicontinuous Cubic Phases of Lyotropic Liquid-Crystals. *Langmuir* 11, 334-340.
- Thurmond, R.L., Lindblom, G., Brown, M.F., 1993. Curvature, order, and dynamics of lipid hexagonal phases studied by deuterium NMR spectroscopy. *Biochemistry* 32, 5394-5410.
- Tiddy, G.J.T., 1980. Surfactant-Water Liquid-Crystal Phases. *Physics Reports-Review Section of Physics Letters* 57, 2-46.
- van Meer, G., Voelker, D.R., Feigenson, G.W., 2008. Membrane lipids: where they are and how they behave. *Nat Rev Mol Cell Biol* 9, 112-124.

Winterhalter, M., Helfrich, W., 1992. Bending elasticity of electrically charged bilayers: coupled monolayers, neutral surfaces, and balancing stresses. *J. Phys. Chem. B* 96, 327-330.